

## Introduction

Beside antenna phase center corrections (PCC) for phase measurement, which are necessary for high accuracy application, there also exist codephase center correction (CPC). These corrections are antenna delays of the code which vary with azimuth and elevation and can reach up to several dm. The estimation approach for CPC from the Institut für Erdmessung (IfE) as well as the validation by receiver-to-receiver single differences (SD) on the observation domain and a simulation of the impact in positioning domain by using a single point positioning (SPP) approach will be shown here.

## Method and estimation approach

- ▶ Antenna under test is rotated and tilted precisely with IfE robot (Fig. 1) around specific point (SP) with distance  $d$  from antenna reference point (ARP).
- ▶ Most effects cancelled out by using:
  - ▶ Short baseline ( $\sim 8$  m) and common-clock set up between reference antenna and antenna under test and
  - ▶ Time differenced single differences ( $\Delta SD$ ).
- ▶ Robot pose has to be modelled.
- ▶  $\Delta SD$  only contains CPC from antenna under test and unmodelled effects/noise  $\epsilon$ :

$$\Delta SD = \Delta CPC_A^k(t_i, t_{i+1}) + \epsilon(t_i, t_{i+1}) \quad (1)$$

Estimation approach by spherical harmonics (eq. 2) with degree 8 and order 8, reads

$$CPC(\alpha^k, z^k) = \sum_{m=1}^{m_{max}} \sum_{n=0}^m \tilde{P}_{mn}(\cos(z^k)) (a_{mn} \cos(n\alpha^k) + b_{mn} \sin(n\alpha^k)) \quad (2)$$

- ▶ Restricting coefficients to zero, where index sum is uneven.
- ▶ Estimated parameters  $\hat{a}_{mn}$  and  $\hat{b}_{mn}$  are inserted into eq. 2 to calculate the CPC grid.
- ▶ Estimation of codephase center offset (PCO) from CPC grid. The residuals indicate the codephase center variations (PCV).

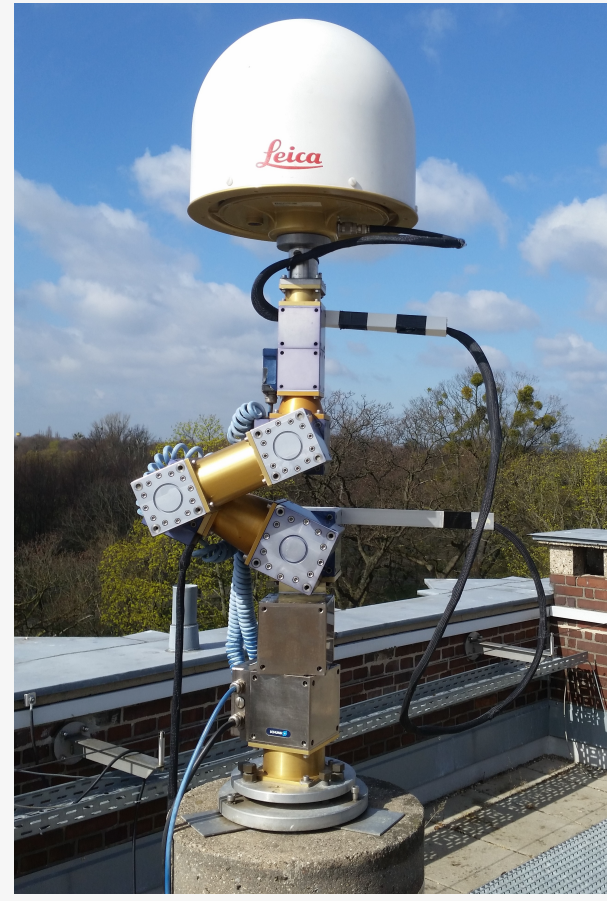


Figure 1: IfE robot for absolute antenna calibration.

## Estimated CPC pattern for different antennas

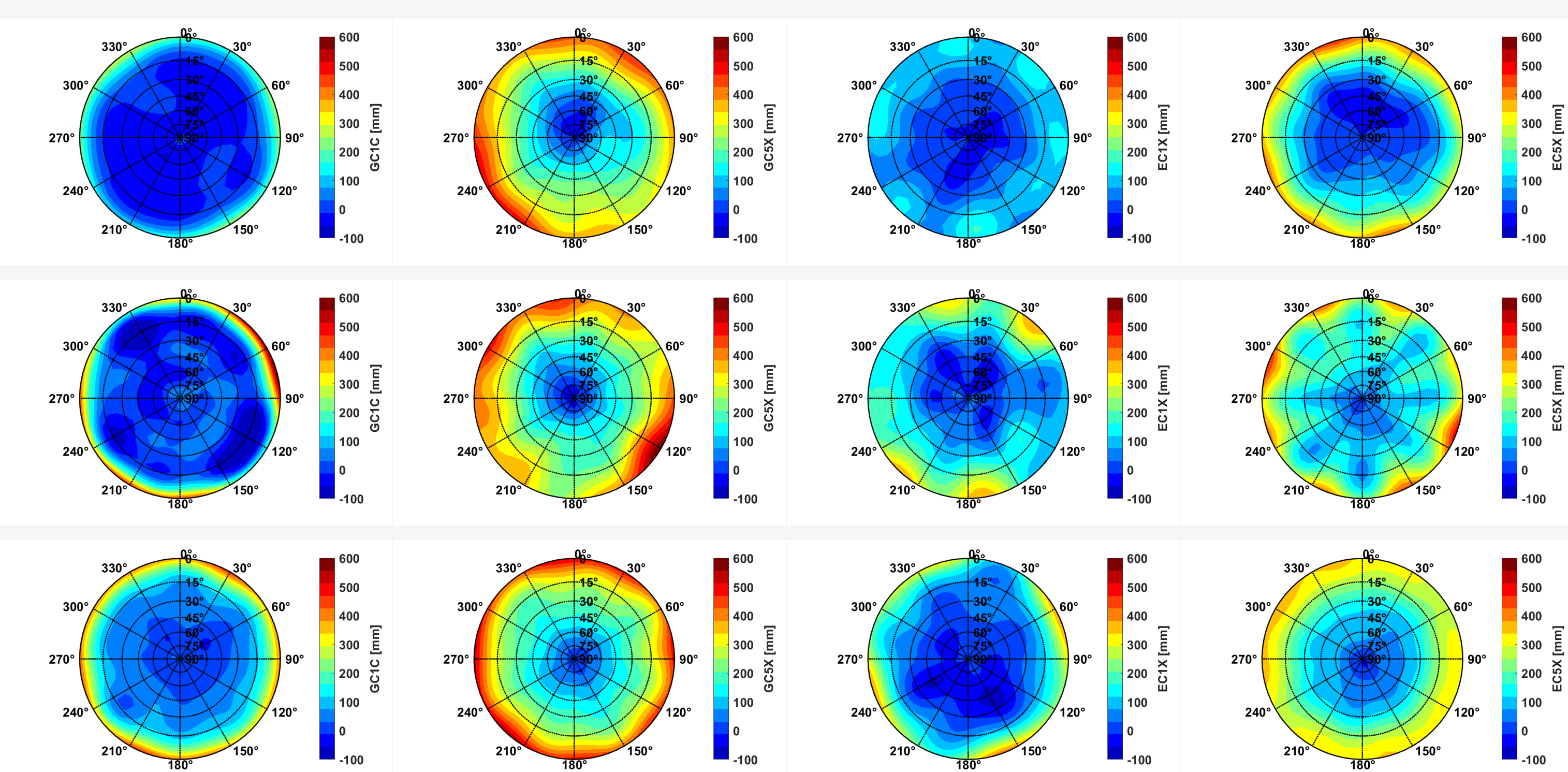


Figure 2: CPC pattern for LEIAR25.R3 LEIT (S/N: 9330001) (top), LEIAR20 LEIM (S/N: 22100016) (middle) and LEIAR20 NONE (S/N: 22100016) (bottom). GNSS signals from left to right GC1C, GC5X, EC1X and EC5X.

- ▶ Fig. 2 shows CPC pattern from different GNSS codephase signals and different antennas.
- ▶ For LEIAR25.R3 LEIT and LEIAR20 LEIM/NONE the CPC varies from -10 cm to 60 cm.
- ▶ C1 patterns shows less variations than C5 patterns especially at higher elevations.
- ▶ The typical similarity within the same frequency between GPS and Galileo PCC pattern<sup>1,2</sup> can not be clearly seen for CPC.

## Repeatability of CPC Pattern

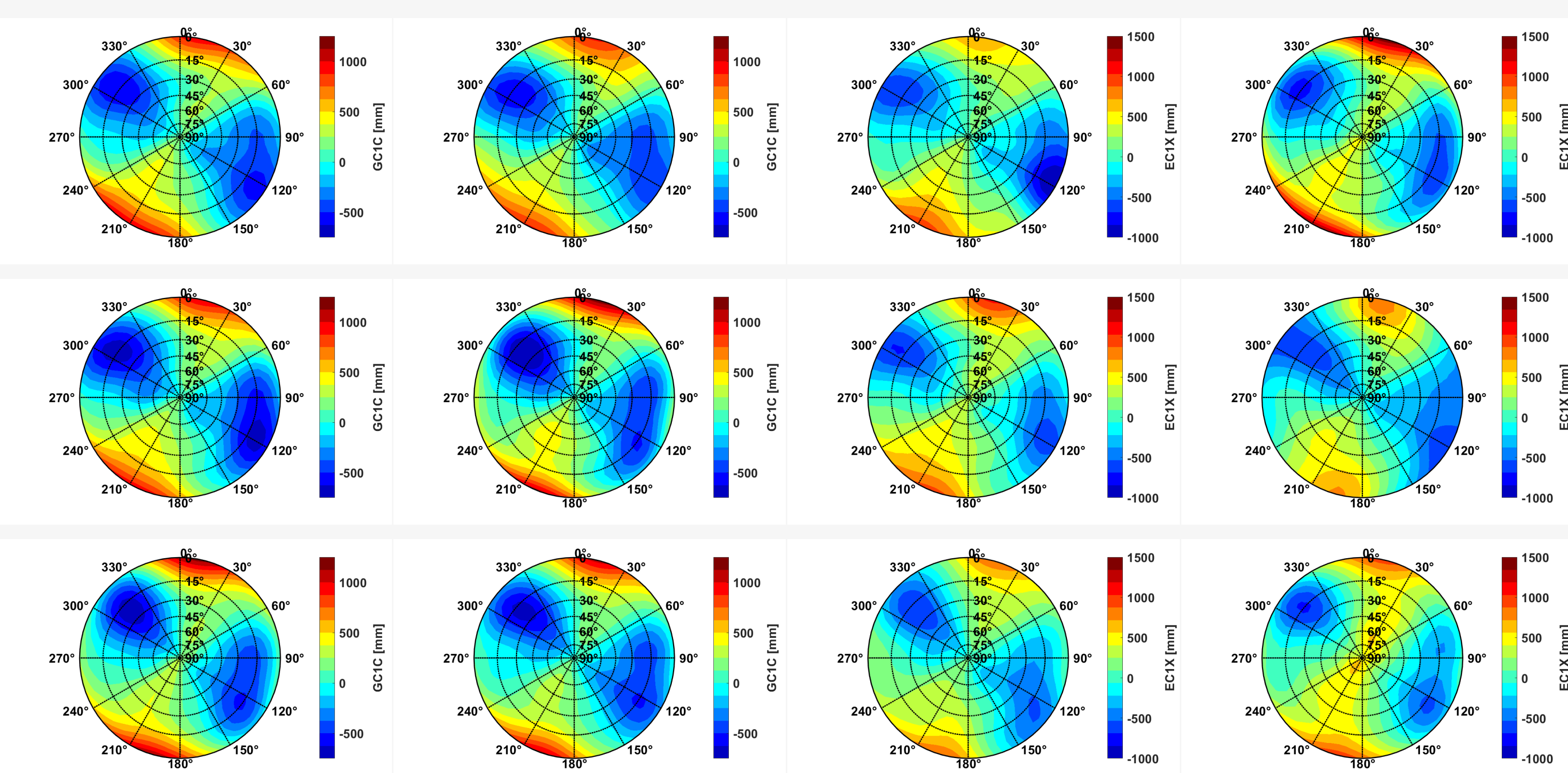


Figure 3: Estimated CPC pattern for the ANN\_MS antenna for the GPS GC1C signal (left six figures) and the Galileo EC1X signal (right six figures). The top row show the CPC from DOY182 and DOY183. The DOY184 and DOY185 are shown in the middle row and the bottom figures represent the pattern from DOY189 and DOY190.

- ▶ Six days of calibration for the ANN\_MS antenna (Fig.4) from July 1<sup>st</sup> to 4<sup>th</sup> and July 8<sup>th</sup> to 9<sup>th</sup> 2019.
- ▶ Fig. 3 shows CPC pattern for GPS signal GC1C (left) and Galileo EC1X (right). The CPC includes the PCV as well as the PCO.
- ▶ Azimuthal variations between -1 m to +1.5 m for the ANN\_MS antenna.
- ▶ Average RMS by consider all possible CPC pattern combination is 8.7 cm for GC1C and 20.5 cm for EC1X.

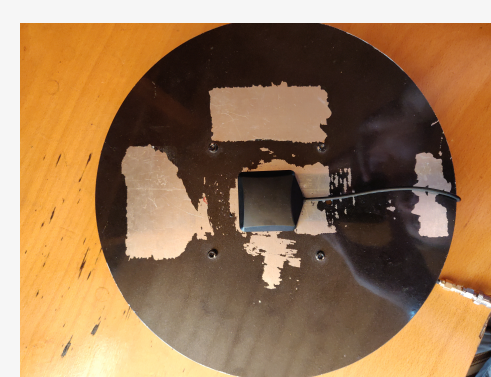


Figure 4: ANN\_MS antenna.

## Validation set-up

- ▶ Experimental set-up on the rooftop of the Geodetic Institute Hannover (GIH) (Fig. 5). Two different antennas (LEIAR25.R3, ANN\_MS) are mounted on two pillars in a common-clock short baseline ( $\sim 26$  m) set-up.
- ▶ The antennas are connected to two Javad Delta receivers, which are also linked to an external rubidium frequency standard.
- ▶ Precise coordinates for the pillars are provided from a network solution 2018 with sub-millimeter accuracy.
- ▶ 1 Hz GPS and Galileo code measurements from July 10<sup>th</sup> to July 12<sup>th</sup> 2019.
- ▶ Calculated SD (0° cutoff) and SPP (3° cutoff,  $\cos(z)$  weighting) are related to antenna ARP.

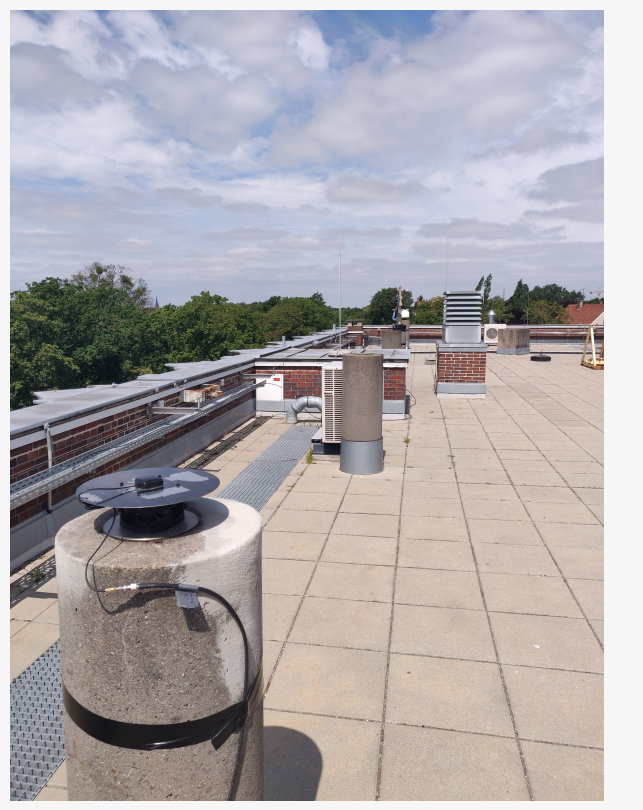


Figure 5: Experimental setup on the rooftop from GIH

## Validation in observation domain

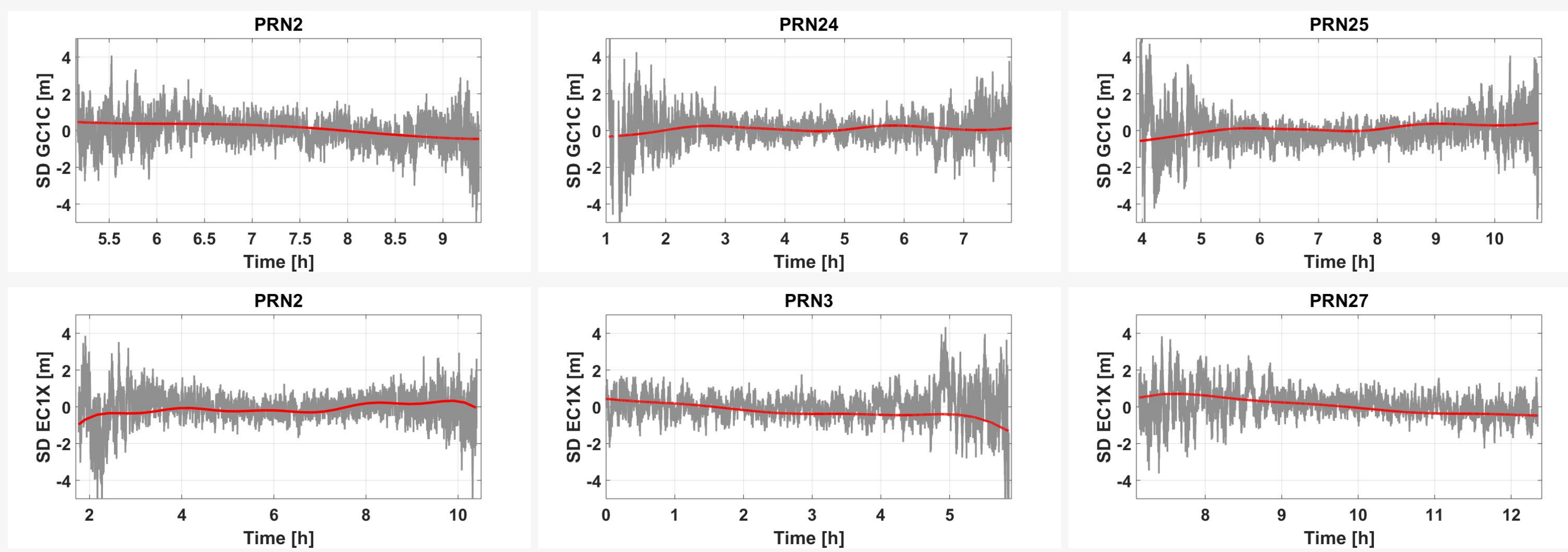


Figure 6: Single differences (grey) from July 12<sup>th</sup> w.r.t. to ARP, without CPC for GPS satellites PRN2, PRN24 and PRN25 (top) and Galileo satellites PRN2, PRN3 and PRN27 (bottom). The GPS signal GC1C and the Galileo signal EC1X are shown. The red curve indicates the CPC estimated by IfE (robot).

- ▶ SD shows expected values, with higher variations at the beginning and the end of observation arcs, which indicates multipath effects.
- ▶ To calculate the CPC the pattern from April 29<sup>th</sup> 2019 (Fig. 2 (top)) is used for the Leica antenna and the pattern from July 1<sup>th</sup> (Fig. 3) is used for the ANN\_MS antenna.
- ▶ The long periodic trends, which are obvious in the SD, can be represented very well with the CPC estimated by IfE (robot).

## Impact of CPC in positioning domain

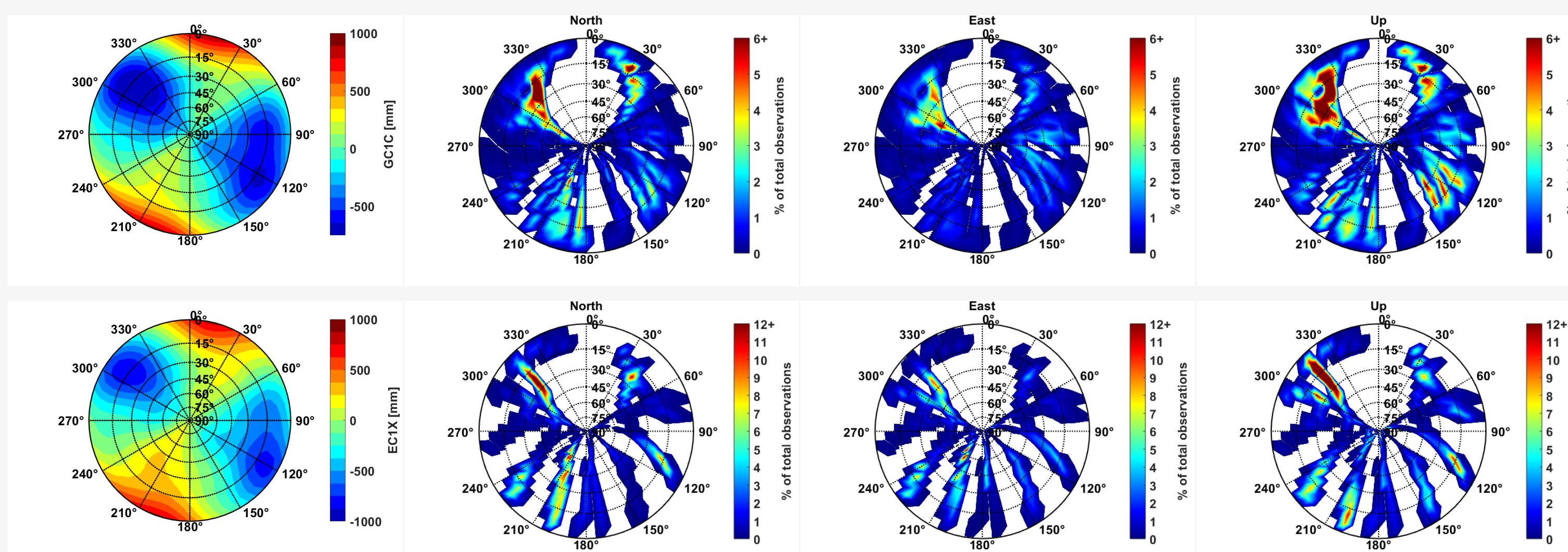


Figure 7: Average impact of CPC on topocentric component for GC1C (top) and EC1X (bottom) for nearly 12 hours data. Mean estimated CPC Pattern from ANN\_MS antenna (left) and the impact in North, East, Up direction (left to right) are shown. The colors define the amount of observation within a pattern bin ( $5^\circ \times 5^\circ$ ) in percent. The highest amount is about 12 percent.

Fig. 7 shows the impact of each CPC  $5^\circ \times 5^\circ$  grid cell on the SPP positioning. To this end, the  $n_{epo} \times n_{cell}$  matrix  $DX(t) = (A^T P A)^{-1} A^T P \cdot M \cdot CPC_{grid}$  is evaluated for each parameter and epoch. Subsequently, the relative contribution of each observation to the coordinate component is computed as a percentage and then averaged over the whole observation period. Finally, the matrix elements are again represented as a skyplot. The plots show particular regions on the antenna, which have more impact on the topocentric coordinates (red) than other regions (blue). The impact from Galileo pattern has higher impact due to less satellites (fig. 9) than GPS. Moreover more regions of the Galileo CPC are not used, due to less satellites as well. Fig (8) shows the impact of the CPC for the ANN\_MS antenna in position domain over 12 hours data. It is visible, that the effect is higher in North and Up direction than in East direction. The effect can reach up to one meter.

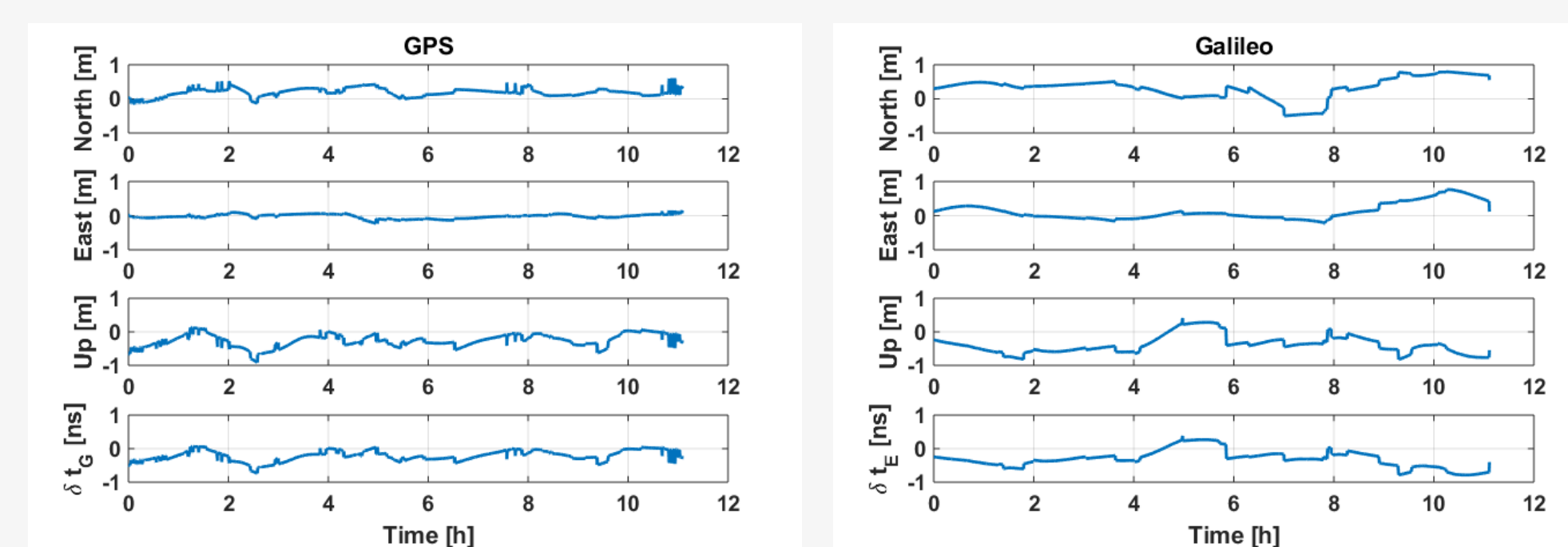


Figure 8: CPC in positioning domain for the ANN\_MS antenna in North, East and Up components as well as the receiver clock residuals.

Figure 9 shows HDOP, VDOP and number of visible satellites. The plots show particular regions on the antenna, which have more impact on the topocentric coordinates (red) than other regions (blue). The impact from Galileo pattern has higher impact due to less satellites (fig. 9) than GPS. Moreover more regions of the Galileo CPC are not used, due to less satellites as well. Fig (8) shows the impact of the CPC for the ANN\_MS antenna in position domain over 12 hours data. It is visible, that the effect is higher in North and Up direction than in East direction. The effect can reach up to one meter.

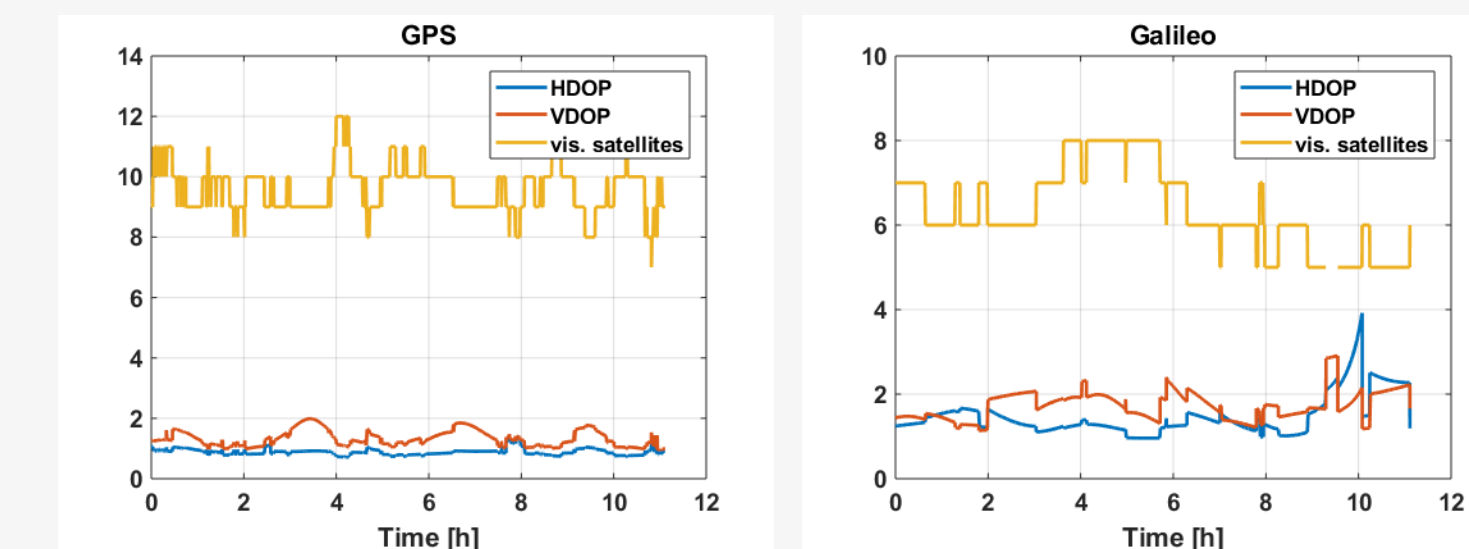


Figure 9: HDOP, VDOP and number of visible satellites.

## Conclusion

- ▶ The repeatability of IfE estimation approach shows an average RMS for GC1C 8.7 cm and for EC1X of 20.5 cm. Due to the not daily sidereal repeatability of Galileo satellites orbits, the higher RMS could be explained.
- ▶ CPC shows long periodic trends in observation and positioning domain.
- ▶ The impact of CPC in position domain shows an effect up to one meter.
- ▶ Not every CPC has the same impact on the different topocentric components. There are regions of the antenna, which have more impact on the estimated position than other regions.

## References

- 1 Breva et al. (2019). Validation of phase center corrections for new GNSS signals obtained with absolute antenna calibration in the field. In: *Geophysical Research Abstracts* 21, 7-12 April, 2019, Vienna, Austria.
- 2 Kröger et al. (2019). Phase Center Corrections for new GNSS signals. In: *Geophysical Research Abstracts* 21, 7-12 April, 2019, Vienna, Austria.